

## BEAM LOSS STUDIES IN THE CSNS LINAC\*

J. Peng<sup>1,†</sup>, Y. L. Han<sup>1</sup>, Z. P. Li<sup>1</sup>, Y. Li<sup>1</sup>, Y. Yuan<sup>1</sup>, X. B. Luo<sup>1</sup>, X. Y. Feng<sup>1</sup>, X. G. Liu<sup>1</sup>,  
 M. Y. Huang<sup>1</sup>, S. Y. Xu<sup>1</sup>, H. C. Liu<sup>1</sup>, S. Wang<sup>1</sup>, S. N. Fu<sup>1</sup>

Institute of High Energy Physics, Chinese Academy of Sciences, Beijing, China

<sup>1</sup> also at Spallation Neutron Source Science Center, Dongguan, China

### Abstract

The China Spallation Neutron Source (CSNS) accelerator consists of an 80 MeV linac and a 1.6 GeV rapid cycling synchrotron. It started operation in 2018, and the beam power delivered to the target has increased from 20 kW to 140 kW, step by step. Various beam loss studies have been performed through the accelerator to improve the beam power and availability. For the CSNS linac, the primary source of the beam loss is the halo generated by beam mismatches. In the upgrade plan of the CSNS, the beam current will increase five times, which requires more strict beam loss control. Much work is done during the design phase to keep the loss down to 1 W/m of loss limit. This paper will report results obtained from beam experiments and optimization methods applied to the CSNS linac upgrade design.

### INTRODUCTION

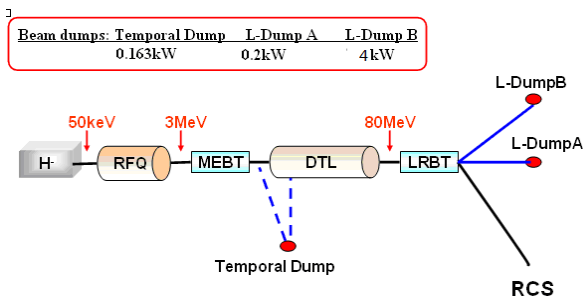


Figure 1: CSNS linac layout.

The CSNS is designed to accelerate proton beam pulse to 1.6 GeV at a 25 Hz repetition rate while striking a solid metal target to produce spallation neutrons. The accelerator aims to provide 100 kW of proton beam power with more than 90% reliability. The accelerator complex consists of an 80 MeV H- linac as the injector and a 1.6 GeV rapid cycling proton synchrotron (RCS), as shown in Fig. 1[1]. The linac consists of a 50 keV H- ion source, a 3 MeV RFQ, an 80 MeV DTL, and several beam transport lines. Table 1 shows the main parameters of the CSNS linac. The beam commissioning of the accelerator was started in 2015, and the first neutrons were produced in 2017. In the following year, the facility was put into user operation with a beam power of 20 kW. Over the next six years, the beam power was gradually improved from 20 kW to 140 kW, which is about 40% more than the design value. Figure 2 shows the beam

power evolution of the CSNS accelerator since the beginning of operation in 2018. During the process of beam power ramping, the peak beam current transporting through the linac has been increased from 10 mA to 15 mA, and the pulse width has been widened from 100  $\mu$ s to 540  $\mu$ s. According to the latest measurement, residual radiation at 30 cm is less than 7mrem/hour throughout the linac, showing that the beam loss level keeps under 1 W/m. During beam commissioning and operation, several problems have been studied and solved, including ion source instability [2], quad failures in the DTL [3], chopping effect, and instability of the LLRF system [4]. These problems can induce beam transmission decline or create large beam loss spots along the linac. There are many H<sup>-</sup> beam loss mechanisms for H<sup>-</sup> accelerators, including residual gas stripping, H<sup>+</sup> capture and acceleration, intra-beam stripping mechanism, and so on [5]. For the CSNS linac, emittance growth arises from the mismatch, and the beam halo is the primary source of beam loss.

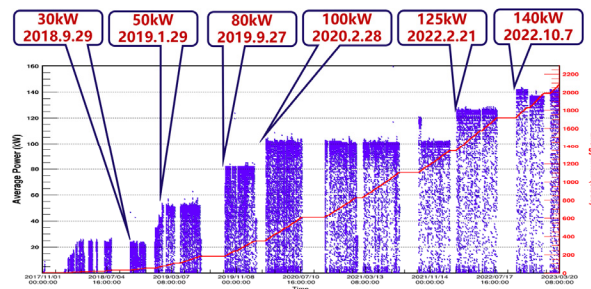


Figure 2: CSNS beam power evolution.

Table 1: Main Parameters of the CSNS Linac

	Ion Source	RFQ	DTL
Input Energy (MeV)		0.05	3.0
Output Energy (MeV)	0.05	3.0	80
Pulse Current (mA)	20	10	10
RF frequency (MHz)		324	324
Chop rate (%)		50	50
Duty factor (%)	1.3	1.05	1.05
Repetition rate (Hz)	25	25	25

### BEAM LOSS STUDIES

#### Ion Source Instability

Before September 2021, the type of Penning IS was used for the CSNS accelerator to produce H<sup>-</sup> beam. At the be-

\*Work supported by National Natural Science Foundation of China (11505201)

†pengjun@ihep.ac.cn

gining of operation, although the beam current met the requirement of the accelerator, the stability was not satisfactory during beam commissioning and operation. This instability caused beam orbit and emittance fluctuation, and the RFQ transmission was affected by the ion source instability. Furthermore, the beam parameters output from the RFQ were changed. As a result, the beam was mismatched while transported in the DTL and then lost in the DTL [6]. During operation, the beam transmission of the DTL might be reduced about 2~4% compared to the value obtained by careful beam commissioning. To solve that problem, we performed many improvements on the ion source. The electric Penning magnet, the post-acceleration ceramic insulator, and the post-acceleration power supply were all replaced by modified ones. It was also found that the instability could be well controlled by strictly limiting the consumption of cesium. After these improvements, the beam transmission fluctuation in the DTL could be kept within 1%.

For the beam power upgrade, in the summer of 2021, the penning ion source was replaced by the RF-driven H<sup>+</sup> ion source. This type of ion source could provide a higher beam current and a wider beam pulse. Table 2 shows the beam emittance difference between the two types of ion sources. The measurement was made with a double-slit emittance monitor located in the middle of the MEFT.

Table 2: Twiss Parameters at the Emittance Monitor

	$\alpha$	$\beta$ (mm/pi mrad)	$\epsilon$ Norm.rms (pi mm mrad)
<i>Horizontal</i>			
Penning ion source	-1.59	0.79	0.243
RF ion source	-2.86	1.12	0.202
<i>Vertical</i>			
Penning ion source	0.87	0.76	0.213
RF ion source	0.66	0.44	0.224

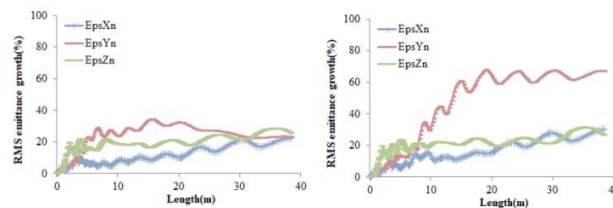
Two groups of the twiss parameters in the vertical plane agree well, while those in the horizontal plane are slightly different.

### Beam halo

For the CSNS linac, the primary source of beam loss is the beam halo or long tails on the beam distribution. When the halo size exceeds the beam pipe, the beam is lost. Beam halo mainly arises from beam mismatch, structure resonances, parametric resonances, and so on.

Sometimes, the amplitudes of the accelerating cavities may be adjusted to lower than nominal settings due to sparking, like the situation in the RFQ. It will cause beam energy deviation and also beam mismatch. A significant beam loss could be observed at the exit of the DTL.

Except for the beam energy deviation, some quadrupole failures could cause beam mismatch, too. Electrical magnet quadrupoles are arranged as the FFDD lattice for the DTL to provide transverse focusing. During the operation, a quadrupole in the 1st DTL tank was turned off due to the leaking of the cooling channels in the drift tube. We have exchanged the polarities of the quadrupoles after the failure magnet and modified the settings of the adjacent quadrupoles to make the transverse phase advance per meter smooth. With those modifications, the beam transmission and beam loss throughout the linac were both recovered. However, since the discontinuity of the transverse focusing, the emittance growth was more significant than those with the nominal magnet settings. Figure 4 shows the simulated RMS emittance growth for two situations. At the exit of the DTL, the vertical emittance growth is 23.2% for the nominal lattice, while the value is 67.1% for the modified lattice, as shown in Figure 3.



(a) Nominal lattice (b) Modified lattice  
 Figure 3: RMS emittance evolution along the DTL

The difference between the computer model and the real machine is also an important source causing beam mismatch. We optimized the magnet model in the MEFT and the DTL to improve the accuracy. Take the magnet in the MEFT, for example; the aspect ratio of the quadrupole is 1.67, which induces an unavoidable fringing field effect, and the simplified hard-edge model was unsuitable. A refined model called the equivalent hard-edge model was adopted[6]. For each magnet, its measured magnetic field distribution was cut into nine thin slices. An equivalent hard-edge model was obtained to make the transfer matrix equal to the product of the transfer matrices of the slicing model. In the beam experiment, the beam parameters at the RFQ exit were measured with the refined hard-edge model, which is much closer to the RFQ design value than the simplified hard-edge model.

### FD vs. FFDD

After the beam power is raised to the design value of 100 kW, the CSNS-II program for accelerator power upgrade to 500 kW will be launched. The output beam energy will be increased to 300 MeV by installing additional SC cavities after the normal conducting linac. The peak current transporting through the linac must be raised from 10 mA to 50 mA. It is rather challenging to complete this purpose because the bore radius of the DTL was designed for a beam current of 30 mA initially. A plan to replace the existing FFDD lattice in the DTL with FD lattice has been considered to solve this problem.

Figure 4 shows the gradients of quadrupole in the DTL. It is shown that the gradients for FD lattice are much higher than those for FFDD lattice. Experiments have been performed that test the feasibility of operating quadrupoles at high gradients. Figure 5 shows the RMS emittance evolution along the linac. It is shown that the emittance growth with FD lattice is slightly less than that with FFDD lattice.

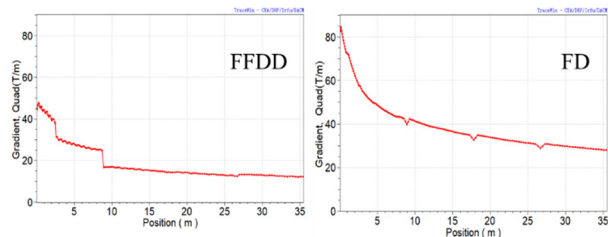


Figure 4: Gradients of quadrupole in the DTL

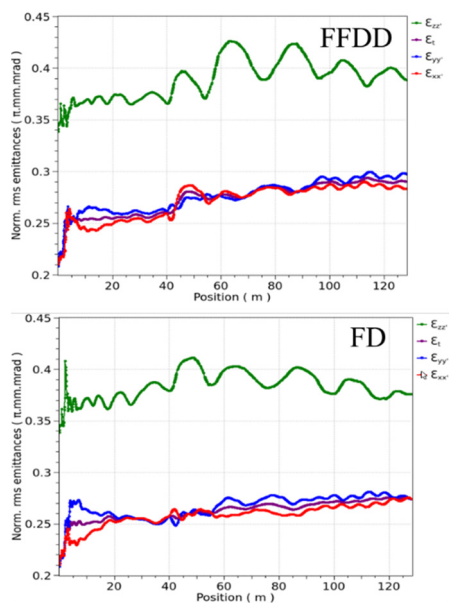


Figure 5: RMS emittance evolution along the MEBT+DTL+SC( $I_{\text{peak}}=50$  mA)

## CONCLUSION

In the paper, we reviewed some issues that could induce beam transmission decline throughout the linac. As we gained more experience from the operation, we modified some elements and adjusted the settings to make the accelerator availability higher than 90%. However, the beam current will have to enlarge nearly five times in the beam power upgrade project. The substantial space charge effect will cause beam halo and emittance growth. The e-P instability will become an obvious issue and cause significant beam loss. Some experiments are planned to study the beam loss mechanisms and find solutions to limit the beam loss along the linac.

## REFERENCES

- [1] S.N. Fu and H.S. Chen, “Status of CSNS Project”, in *Proc. IPAC'13*, Shanghai, China, May 2013, paper FRXAB201, pp. 3995-3999.
- [2] H.F. Ouyang and X. Cao, “The operation status of CSNS front end”, in *Proc. IPAC'19*, Melbourne, Australia, May 2019, pp. 2024-2026.  
doi:10.18429/JACoW-IPAC2019-TUPTS038
- [3] J. Peng and Y.W. An, “Beam dynamics studies for the CSNS DTL due to a quadrupole fault”, in *Proc. LINAC'18*, Beijing, China, 16-21 Sep. 2018, pp. 573-575.  
doi:10.18429/JACoW-LINAC2018-TUP0114
- [4] Zhencheng Mu and Jian Li, “Overview of the CSNS Linac LLRF and operational experiences during beam commissioning”, in *Proc. HB'16*, Malmö, Sweden, Jul. 2016, pp. 409-412.  
doi:10.18429/JACoW-HB2016-WEAM2Y01
- [5] M. Plum, “Beam Loss in Linacs”, Proceedings of the Joint International Accelerator School: Beam Loss and Accelerator Protection, Newport Beach, US, 5–14 November 2014, edited by R. Schmidt, CERN-2016-002 (CERN, Geneva, 2016).  
doi:10.48550/arXiv.1608.02456v1.
- [6] Luo X and Peng J, “Study on the fringe field effect of quadrupoles for CSNS MEBT”, *Radiation Detection Technology and Methods*, vol. 7, no. 1, pp. 134-138, 2022.  
doi:10.1007/s41605-022-00359-9.